J. Phys. A: Math. Theor. **46** (2013) 065002 (14pp) doi:10.1088/1751-8113/46/6/065002

Comparing the results of lattice and off-lattice simulations for the melt of nonconcatenated rings

Jonathan D Halverson[1], **Kurt Kremer**[2] **and Alexander Y Grosberg**[3]

[1] Brookhaven National Laboratory, Center for Functional Nanomaterials, Upton, NY 11973, USA
[2] Max Planck Institute for Polymer Research, Ackermannweg 10, D-55128 Mainz, Germany
[3] Department of Physics and Center for Soft Matter Research, New York University, 4 Washington Place, New York, NY 10003, USA

E-mail: jhalverson@bnl.gov, kremer@mpip-mainz.mpg.de and ayg1@nyu.edu

Received 21 August 2012, in final form 20 December 2012
Published 28 January 2013
Online at stacks.iop.org/JPhysA/46/065002

Abstract
To study the conformational properties of unknotted and nonconcatenated ring polymers in the melt, we present a detailed qualitative and quantitative comparison of simulation data obtained by molecular dynamics simulation using an off-lattice bead-spring model and by Monte Carlo simulation using a lattice model. We observe excellent, and sometimes even unexpectedly good, agreement between the off-lattice and lattice results for many quantities measured including the gyration radii of the ring polymers, gyration radii of their subchains, contact probabilities, surface characteristics, number of contacts between subchains, and the static structure factors of the rings and their subchains. These results are, in part, put in contrast to Moore curves, and the open, linear polymer counterparts. While our analysis is extensive, our understanding of the ring melt conformations is still rather preliminary.

PACS numbers: 61.41.+e, 61.25.he, 87.16.Sr

(Some figures may appear in colour only in the online journal)

Motivated in part by the exciting applications in the genome folding problem [1–5] and partly by materials science questions [6–8], we have recently undertaken several studies of conformational and dynamical properties of very concentrated systems of nonconcatenated (unentangled) ring polymers [9–12]. Our purpose here is to compare the results obtained by Monte Carlo simulation for a cubic lattice model of nonconcatenated rings [9] with those obtained by molecular dynamics simulation (off-lattice) [10–12]. Although qualitative similarities, as expected by universality considerations [13], are quite obvious and were pointed out in the original publications, the quantitative comparison was not undertaken before. In addition we compare our data to a closed loop Moore curve, which is a recursively constructed space filling fractal curve [14, 15]. Moore curves are unknotted, globular and self-segregating on a hierarchy of scales, making them excellent reference cases when considering

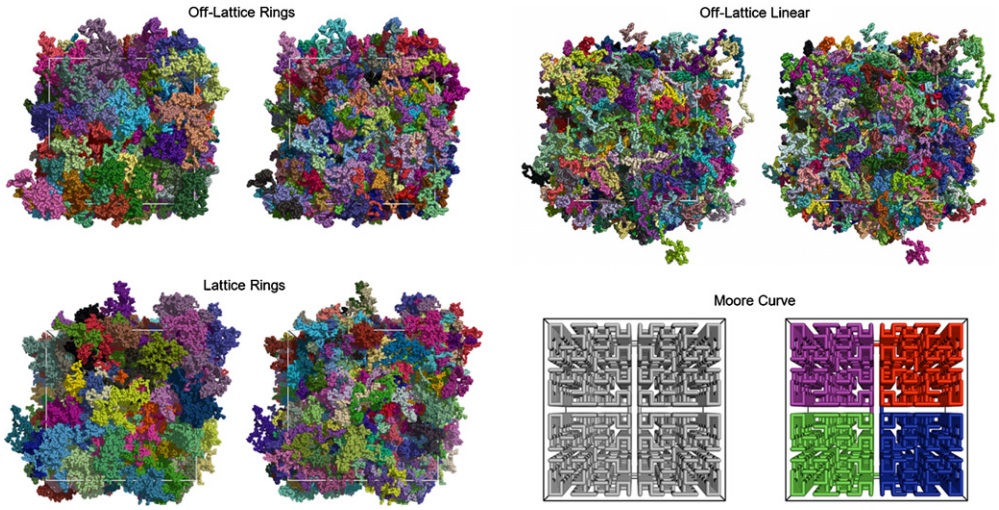

Figure 1. The off-lattice rings (upper left) and on-lattice rings (lower left) behave as 'territorial polymers.' That is, when each polymer in the system of nonconcatenated and unknotted rings is colored with its own color, an image emerges that is similar to a political map of some unknown continent. For the off-lattice system the image shows 200 rings of $N = 1600$ monomers each while for the lattice system there are 142 rings with $N = 10082$. The 'territorial segregation' property is not only observed for entire rings (left image of each case), but also for their subchains (right images). In the latter case, every quarter of every chain in the melt (400 monomers in the off-lattice case versus about 2520 in the lattice case) was colored with its own color and once again partial segregation is observed. This is in contrast to the linear polymers of length $N = 800$ (upper right) which do not show any significant segregation for either coloring scheme. The Moore curve shown for $N = 4096$ (lower right) resembles a ring in the melt because of its closed topology and the segregation of its subcurves, which is quite pronounced.

ring conformations. Space filling curves have previously been considered in the context of the genome folding problem, see e.g. the supplementary material of [1].

Qualitatively, the main observation for both lattice [9] and off-lattice [10–12] models is that nonconcatenated rings segregate from one another. That means that each ring gets to a certain extent compacted or squeezed between neighboring rings. Obviously, each ring prefers to lose some entropy by shrinking in order to avoid losing even more entropy by penetrating the surrounding long loops. The very phenomenon of segregation between nonconcatenated rings is observed for both the lattice and off-lattice systems (see left column of figure 1). This is in contrast to linear polymers in the melt which interpenetrate and do not form territories.

With respect to the quantitative features of ring conformations in the melt, we will discuss the overall size scaling and its exponent ν, then contact probability exponent γ, surface roughness exponent β (and variations thereof), static structure factor scaling, and the relations between these quantities.

Let us first consider the overall size of a ring in the nonconcatenated melt. We have previously presented in [12] the master plot of the mean squared ring gyration radius R_g as a function of ring length N, collecting data from several different computational works. The key idea in the master plot of figure 2 is to rescale the chain length N by the entanglement length N_e, which must be independently determined for every particular model by properly analyzing the melt of linear chains of the same microstructure. This is done by either analyzing stress relaxation and fitting the data directly by the so-called primitive path analysis [16], or by the related packing length criterion. As is seen in the figure legend, the parameter N_e changes over

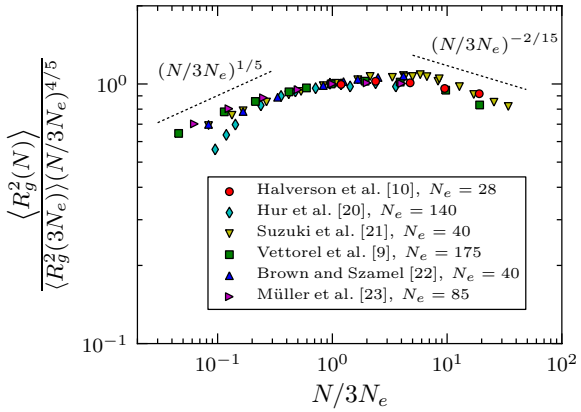

Figure 2. This master plot collects data from a number of different works and shows the dependence of the ring size $\langle R_g^2 \rangle$ on chain length N with the idea that N is taken in ratio to the model-dependent entanglement length of the corresponding linear chains N_e or in this case $N/3N_e$. The ordinate is the mean squared average gyration radius divided by the Cates and Deutsch prediction $N^{4/5}$ [19] (and normalized by the same value at $N = 3N_e$, such that all curves are forced to coincide at $N/3N_e = 1$). Apart from polyethylene chains [20], all data [10, 21, 9, 22, 23] collapse to the master curve which exhibits a very wide crossover from Gaussian behavior $\langle R_g^2(N)\rangle \sim N$ at $N < N_e$ to globular behavior $\langle R_g^2(N)\rangle \sim N^{2/3}$ at $N > 15N_e$. Reproduced from [12]. Copyright 2011 by the American Physical Society.

quite a wide range for different models examined in the literature. In particular, our lattice model [17, 9] has $N_e = 175$, while our off-lattice model [18, 10] has $N_e = 28$, and these incidentally happen to be largest and smallest among the models tested in the literature and collected in figure 2. As a result, the longest rings equilibrated in the lattice model ($N = 5100$) are effectively even somewhat shorter than the longest rings in off-lattice model ($N = 1600$): $N/N_e = 57$ off-lattice versus $N/N_e = 29$ on-lattice ($N = 10082$ was run for the lattice model, but its equilibration was not convincing). The lattice simulations were conducted on a cubic lattice with lattice constant σ. For the off-lattice simulations, the length scale σ enters through the repulsive interaction between beads. However, the average bond length is 0.97σ, which is nearly identical to the lattice case. The squared statistical segment lengths of the off-lattice and lattice models are $b^2 = 2.71\sigma^2$ and $1.90\sigma^2$, respectively. Both systems are simulated under melt conditions, which is a density of occupied sites of 0.5 for the lattice case and $0.85/\sigma^3$ for off-lattice. The off-lattice linear systems have the same density and b^2 as the off-lattice rings. For the Moore curves the bond length is σ.

The vertical axis in figure 2 is chosen such that the Flory-type prediction by Cates and Deutsch [19], $R_g \sim N^{2/5}$, would correspond to a horizontal line. We see that in reality the rings behave as Gaussian, $R_g \sim N^{1/2}$, at $N < N_e$, and approach globular behavior, $R_g \sim N^{1/3}$, at sufficiently large N. At the same time, there is also the unexpectedly wide cross-over range. Encouraged by the simple arguments leading to the theory [19] one might be tempted to declare the behavior of R_g in this cross-over region to be close to the predicted $N^{2/5}$, however, the justification of such a view is very weak because there is a very wide crossover, but never really a plateau.

A more detailed view of the conformations is afforded by looking at the subchain sizes. As a preparation step, we show in figure 3 the gyration radii of the subchains of the linear chains. The subchains are found to follow a Gaussian scaling $\langle R_g^2 \rangle \sim s$ with departure from this behavior at lengths below about 10^2 monomers. The departure is due to the tangent–tangent

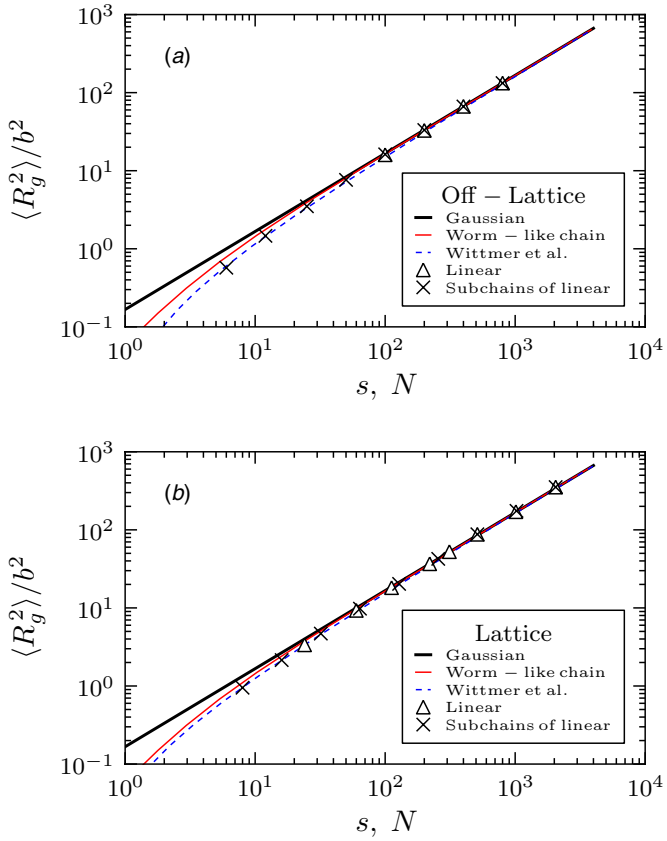

Figure 3. Mean squared gyration radius of linear chains in the melt or their subchains are shown against the length of either the full chains N or subchains s, for both off-lattice and lattice systems. Thick lines correspond to purely Gaussian behavior, $\langle R_g^2\rangle/b^2 = N/6$, thin lines show the result for exact worm-like chain, equation (1), and dashed lines represent the long-range bond–bond correlations in the melt, for the whole chains and subchains, as discovered in [25, 26] and described by equation (2). Symbols indicate our simulation data. The adjustable parameter c is found to be $c = 0.97$ for off-lattice and $c = 0.79$ for lattice systems.

correlations between bonds. In an isolated worm-like macromolecule, such correlations decay exponentially, and this leads to the $\langle R_g^2\rangle$ of s dependence of the form

$$\frac{\langle R_g^2\rangle}{b^2} = \frac{s}{6}\left[1 - \frac{3}{2s} + \frac{3}{2s^2} - \frac{3}{4s^3}(1 - \mathrm{e}^{-2s})\right], \tag{1}$$

indicated as a thin solid line in figure 3. Equation (1) can be easily derived by proper integration based on the well-known result for the end-to-end distance of a worm-like chain, see, e.g., [24]. It is a common misconception that exponential decay of tangent–tangent correlations produces an exponential approach of $\langle R_g^2\rangle/b^2$ to its Gaussian asymptotics $s/6$. In fact, the approach is a power law, $1/s$. In a concentrated system of linear chains, as it was recently discovered in [25, 26] (see also the recent detailed review [27]), there are also slower power-law decaying correlations which lead to a R_g^2 of s dependence of the form

$$\frac{\langle R_g^2\rangle}{b^2} = \frac{s}{6}\left[1 - \frac{c}{\sqrt{s}}\right], \tag{2}$$

with an adjustable parameter c (see also [28]). This dependence is indicated as a dotted line in figure 3. Here, we do not delve deeply into the subject of these corrections. We only point out that they are well understood and, importantly for our present consideration, they look essentially identical for lattice and off-lattice systems.

We are now ready to look at the subchain sizes of the ring polymers and the subcurve sizes of the Moore curves. We have not considered these quantities in our previous work. Figures 4(a) and (b) show the gyration radii of the subchains of the ring polymers as a function of the subchain length s, and compare them with the sizes of full rings and linear chains. Both lattice and off-lattice systems exhibit similar subchain behavior in that short subchains of rings become indistinguishable from linear chains, while longer subchains approach ring behavior. The ratio of $\langle R_g^2 \rangle$ for the linear and ring systems (i.e. the vertical shift between curves in the log–log plots of figures 4(a) and (b)) in the small N range is very close to 2. This is expected because the constraint of having no knots is very weak for rings in the range of small N, so the system is very nearly Gaussian, in which case connecting two ends is well known to lead to size reduction by a factor of $\sqrt{2}$ (see, e.g., section 10 in [24]). With increasing subchain length s, the gap between the sizes of the linear and ring systems widens. This is because connecting two ends becomes a subdominant effect with increasing N, a much stronger shrinking effect kicks in for rings, which is the compression by surrounding rings due to their topological nonconcatenation, something completely absent for linear chains. The 'switch', or cross-over from linear-like behavior at small s to ring-like at larger s starts in the vicinity of $s/N_e \approx 1$ for both lattice and off-lattice systems, which is remarkable given the large ratio of entanglement lengths N_e for the two models close to the factor of $178/28 \approx 6$. Thus, subchains of nonconcatenated rings are relatively compact, but not quite as compact as the rings themselves. For the Moore curves the situation is quite different. The subcurves are larger than the full curves for all N and both show a scaling consistent with a compact object over the entire range of s and N. This is in contrast to the rings which show different scaling regimes with respect to their gyration radii depending on chain length.

The fact that long subchains in rings are rather compact is also seen in the 'geographic maps' of figure 1. If instead of entire rings we color their quarters, we still see that each quarter of a ring occupies its own 'territory' and to some extent it is segregated from the other subchains, as one can see in the right images of each of the four cases of figure 1. For the Moore curve this is much more pronounced, while for the linear polymers, which are largely intermixed to begin with, coloring the subchains has little effect.

An even more detailed characterization of conformations is contained in the static structure factor, which we show in figure 5. In figure 5 we use modified coordinates motivated by the considerations in [29], as shown in our previous paper [10]. We will discuss these data below, after the discussion of the critical exponent β. Here we just point out the remarkable similarity of $S(q)$ for nonconcatenated rings in both lattice and off-lattice systems. In the inset of figure 5 the traditional scaling of static structure factor $S(q)$ against $q\langle R_g^2 \rangle^{1/2}$ is shown for both models, where q as usual is the absolute value of scattering wave vector, and the product $q\langle R_g^2 \rangle^{1/2}$ relies on the idea that R_g is the only relevant length scale. $S(q)$ for the Moore curve (not shown) is quite distinctive from that of the ring polymers. The 'monomers' of the curve compose a finite piece of a simple cubic lattice leading to a Porod law type scattering curve with oscillations and an envelope slope close to q^{-4}.

Let us now consider properties of polymer rings going beyond the scaling exponent ν. The loop factor or equivalently the contact probability, $P(s)$, is the probability of two monomers of the same chain being separated by s bonds and a distance of less than r. This quantity is of particular interest because it is measured for chromatin fibers experimentally by the 'C' methods such as 3C and its modifications up to HiC [1–3]. The results for lattice and off-lattice

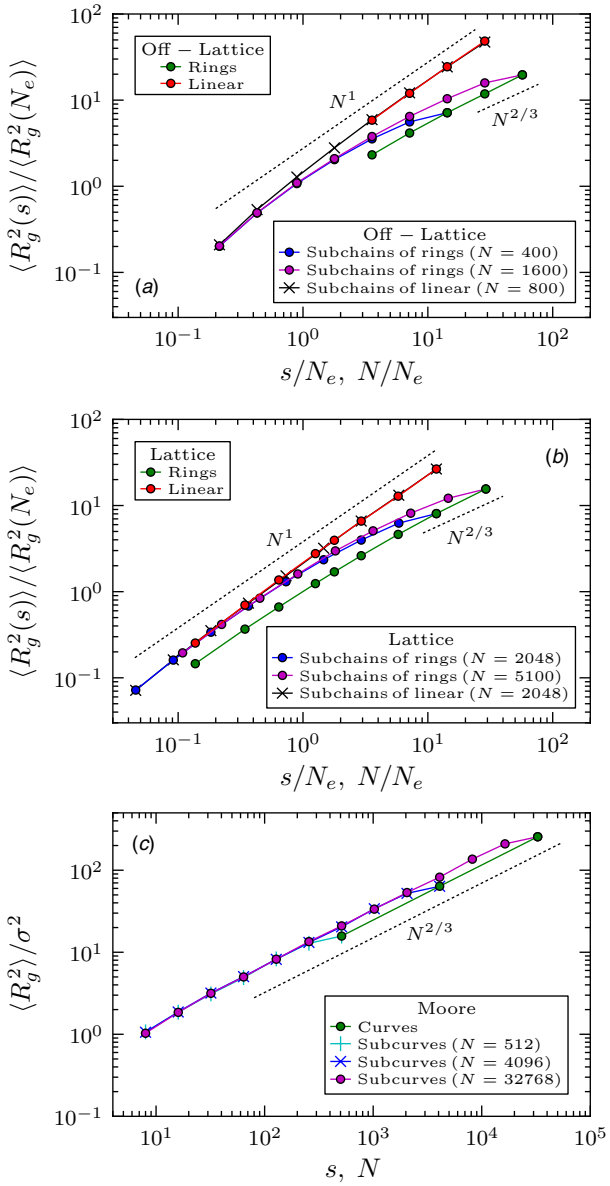

Figure 4. The mean squared gyration radius of subchains of rings in the melt of nonconcatenated, unknotted rings and Moore curves. For the off-lattice systems, we show data for subchains of rings of the lengths $N = 400$ and 1600, while for the lattice systems we consider rings of $N = 2048$ and 5100. For each we examine subchains of the length $s = N/2, N/4, N/8, \ldots$, down to about $s = 6$. For comparison, the data for subchains in the melt of linear chains are reproduced from the figure 3. All data are normalized by $\langle R_g^2(N_e)\rangle$ of the rings which is 7.4 and $25.3\sigma^2$ for the off-lattice and lattice models, respectively. For both ring systems, we see that the size of a short subchain is indistinguishable from that of a linear chain. As the ring subchain gets longer, it becomes more compact in a scaling sense. Importantly, the gap between $\langle R_g^2\rangle$ for a ring subchain and a linear chain widens with increasing s and becomes significantly larger than the factor of 2, which means that the subchain of the ring gets compacted not only because of the connected ends of the ring, but also because of the additional squeezing from the surrounding chains. In contrast, the subchains of the Moore curves from the very beginning by construction follow $\langle R_g^2(s)\rangle \sim s^{2/3}$, with a characteristic drop of the amplitude at the step from $s = N$ to $N/2$.

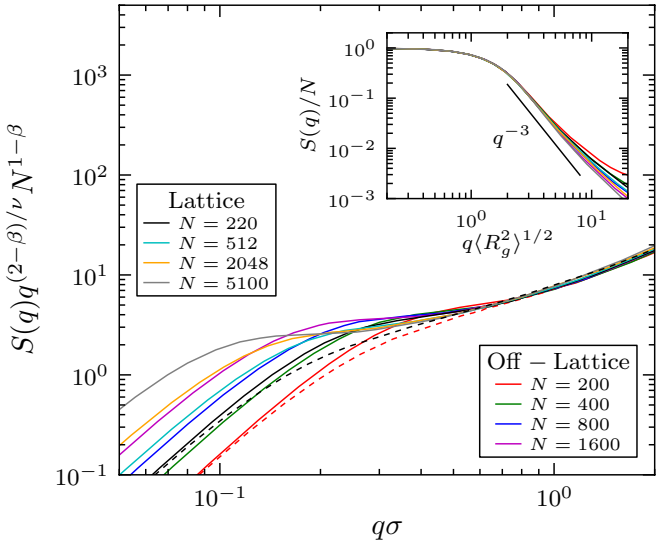

Figure 5. Static structure factor of a single ring in the melt for the off-lattice and lattice systems. The data are plotted in a way that exploits the space-filling nature of conformations, namely, the fact that in a dense melt only the surface between the labeled ring and its unlabeled surroundings contributes to the scattering. This is why the surface roughness exponent β enters the definition. All the data collapse in the relevant range of scattering wave parameter q using the values $\beta = 0.93$ and $\nu = 1/3$. The dashed lines corresponds to a subchain of length s: off-lattice in red with $s = 200, N = 1600$ and lattice in black with $s = 512, N = 5100$. The inset shows the data in the traditional scaling.

models are shown in figure 6(a). There is a close qualitative and quantitative similarity between loop factors of lattice and off-lattice systems despite the different nature of the models. In both cases the contact probability decays with contour length s as $P(s) \sim s^{-\gamma}$, where $\gamma \approx 1.2$.

Lattice and off-lattice data agree well overall but they display different characteristics in approaching the power law region. Though not surprising considering the bare models, this makes it difficult to precisely determine γ. We should point out that this is important in comparison to experimental data on chromatin which are believed to indicate γ close to unity or only slightly larger (e.g., 1.08 for human [1] and 1.05 for mouse [3]). The Moore curve displays a qualitatively different behavior, as shown in figure 6(b). By construction, specific distances display much higher/lower contact probabilities than other nearby contour distances. Because of the recursive construction of the overall curve this does not average out over the whole curve. More subtly, for the ring polymers the value of γ is not trivial to reconcile with various characteristics of surface roughness, which we consider next.

Surface roughness is indeed the natural bridge between the loop factor (or contact probability) with its exponent γ and the 'geographic map' images. As we see in any of the 'political maps' above, although the large rings are segregated in the sense that the gyration radius scales as that of a condensed body, $R_g \sim N^{1/3}$, the surface of any such crumpled ring is by no means smooth. There are several ways to characterize this non-smoothness quantitatively, the simplest one being to count monomers on the surface of every ring in the melt. Here a monomer is said to be on the surface of a ring if it is within a distance r of at least one monomer not belonging to the same ring. For the off-lattice systems we use $r = 2^{1/6}\sigma$,

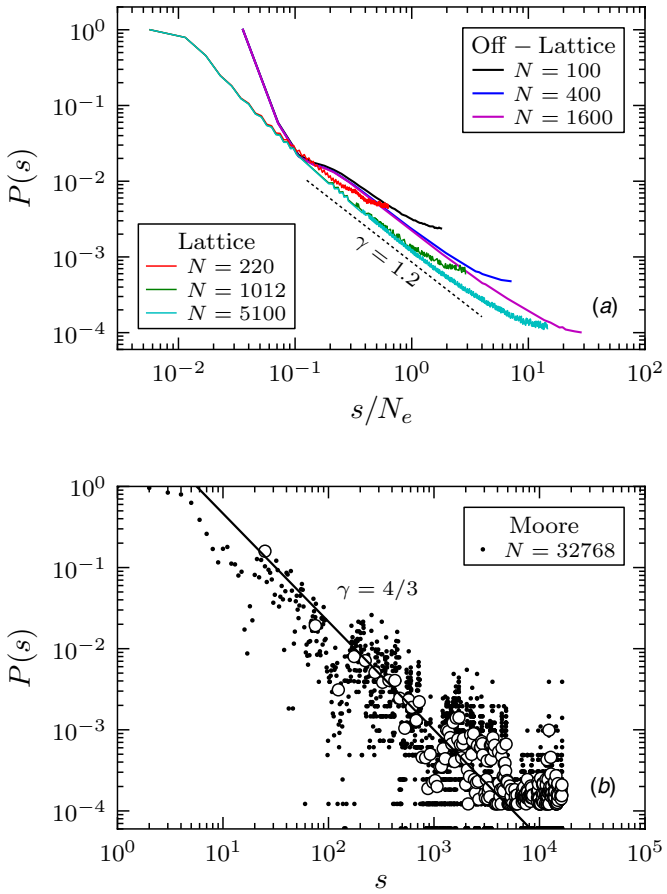

Figure 6. (*a*) The contact probability, or loop factor, as a function of contour length appears to follow a power law $P(s) \sim s^{-\gamma}$ with $\gamma \approx 1.2$ for both the off-lattice and lattice systems. In order to get the data sets to collapse at large s/N_e, the contact defining length r for the off-lattice system was taken as 1.07σ while the lattice system value was $\sqrt{3}\sigma$. (*b*) For the Moore curve there is significant scatter with limiting power laws between $\gamma \approx 1.1$ and $\gamma \approx 1.5$ and a mean around $\gamma = 4/3$. The large unfilled circles correspond to a moving average with a window size of 50 points. Points with $P(s) = 0$ were ignored from the average.

while for the lattice systems and Moore curves $r = \sqrt{3}\sigma$. The number of surface monomers scales as

$$n_{\text{surf}}(N) \sim N^{\beta_1}, \tag{3}$$

with the ring length N. This power β_1 is defined as the first surface roughness exponent. A value of $\beta_1 = 2/3$ implies a completely collapsed object with a smooth surface, while $\beta_1 = 1$ corresponds to a fluffy object whose surface is so rough that it blurs the distinction between surface and bulk.

The dependences of n_{surf} on N are plotted in figure 7 for off-lattice and lattice models. The similarity between the ring systems is striking. In both cases the data follow a power law with surprisingly high accuracy, and in both cases the power β_1 is slightly below unity. Using a least squares fitting procedure which weights the data by the inverse of the statistical error for each point, we found $\beta_1 = 0.97 \pm 0.01$ for lattice rings and $\beta_1 = 0.970 \pm 0.002$ for off-lattice systems. It is so close to unity, that one is naturally tempted to hypothesize it *is* unity, but the

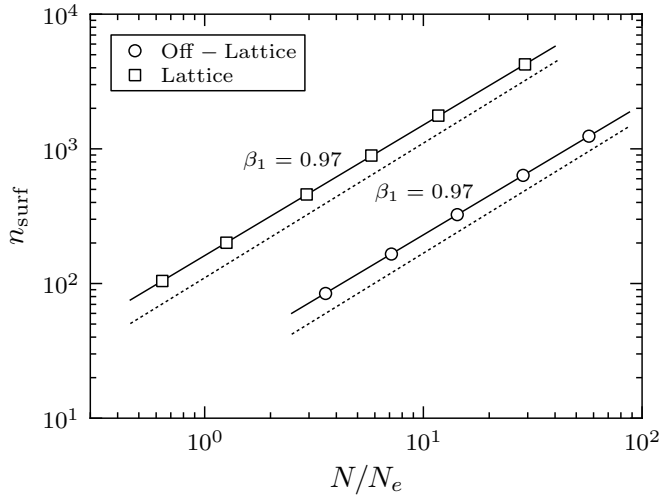

Figure 7. The number of surface monomers per ring as a function of N/N_e. The dependence of $n_{\rm surf}$ on N unexpectedly follows the same power law scaling for both lattice and off-lattice models with $\beta_1 = 0.97$, with error bar not worse than 0.01. The solid lines have been fit to the data. The dashed lines show $n_{\rm surf} \sim N$.

accurate error analysis as indicated above seems to rule this out. What is possible is that the deviation of $n_{\rm surf}$ from linear dependence on N masks a logarithmic correction. However, the fact that $n_{\rm surf}$ follows a power law so accurately for both lattice and off-lattice models makes us cautiously suspect that maybe indeed there is a power law with β_1 slightly below unity. We emphasize here that the same power law is observed at $N/N_e < 1$ and $N/N_e > 1$. In this regard, it is important to measure similarly defined β_1 also for the melt of linear chains. We have done that, and got the result $\beta_1^{(\rm linear)} = 0.99 \pm 0.01$, which is not distinguishable from unity within our current measurement accuracy. Thus, in this regard rings appear to be (slightly) different from linear chains even at $N < N_e$; we leave this observation for now without any interpretation.

In fact, the question of surface roughness deserves a more detailed study. The way we defined the index β_1 above has to do with the 'surface' area of the entire ring of N monomers in the melt where it is surrounded by other rings of the same number of monomers. That means, when we talk about the dependence of $n_{\rm surf}$ on N, we measure how $n_{\rm surf}$ varies from one system to another. We can also look at a possibly different characteristic, namely, the surface roughness of the subchains. While the index β_1 characterizes boundaries between territories in the full ring maps in the left images in figure 1, now we want to examine subchain maps such as the right images of each case in figure 1. Consider a melt of rings of length N, and there look at subchains of the length $s < N$ (more accurately, $s < N/2$). Each such subchain is to some extent crumpled, in the sense that its size is smaller than Gaussian, as we have seen in figure 4.

Specifically, let us consider each ring of N monomers as a system of N/s subchains, or blobs, of length s monomers each. Let us define $n_{\rm surf}(s)$ as the number of monomers in a subchain of length s which have contacts to monomers from other subchains (i.e. from other subchains of the same chain or from other chains), and let us examine the dependence of $n_{\rm surf}(s)$ on s. For this we may assume it is described by the same exponent β_1 as we introduced before (see equation (3)):

$$n_{\rm surf}(s) \sim s^{\beta_1}. \tag{4}$$

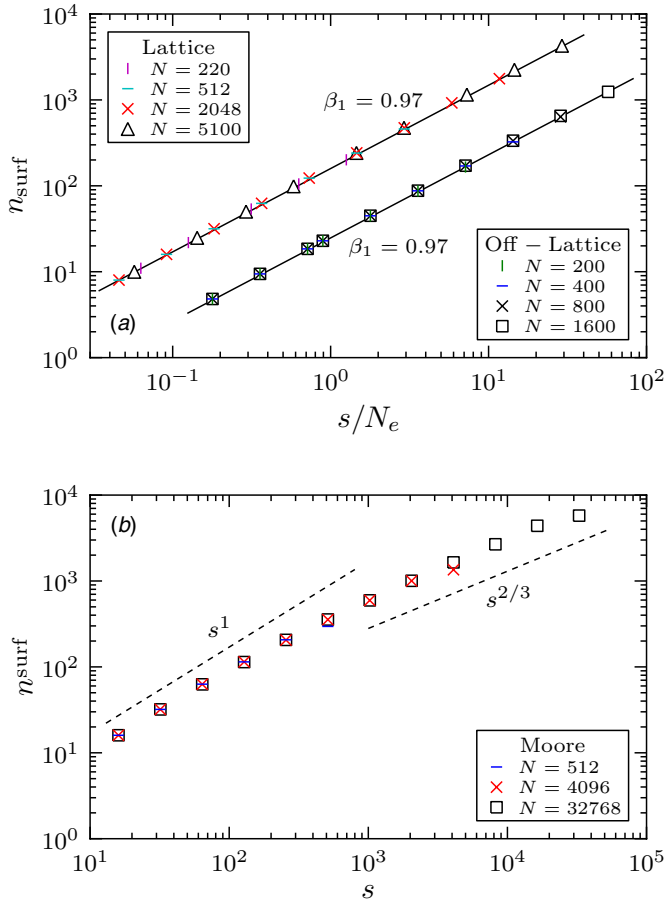

Figure 8. The number of surface monomers of subchains in the ring as a function of subchain length s. The dependence of n_{surf} on s unexpectedly follows a power law for both off-lattice and lattice models quite accurately, while the Moore curve data are qualitatively different. The solid lines in (a) have been fit to the data.

The dependence of n_{surf} on s, for rings of various overall lengths N, is shown in figure 8. We have not considered $n_{\text{surf}}(s)$ in our previous work. As for the entire rings, the value of the exponent is very close to unity ($\beta_1 = 0.97 \pm 0.01$), but it is slightly below unity—and it is most certainly the same as for entire rings (see figure 7). It is also remarkably stable in the sense of being very accurately the same for lattice and off-lattice systems. In contrast to this, the Moore curve data display what one would expect for a compact object. For short pieces $n_{\text{surf}}(s) \sim s^1$, while for longer pieces there is a distinct separation between the bulk of the curve and the surface with $n_{\text{surf}} \sim s^{2/3}$, corresponding to a dimensionality of the surface of $d_{\text{surf}} = 2$.

In the [10], we gave an argument suggesting that there should be an exact relation between exponents of contact probability γ and surface roughness β, namely $\gamma + \beta = 2$. So far, it seems that this relation is not borne out in the data of the rings, while the Moore curve data seem on average to agree to this conjecture. This motivates us to look at yet another

characteristic of surface roughness, namely, the number of monomer–monomer contacts between two contacting blobs

$$n_{\text{blob}-\text{blob}}(s) \sim s^{\beta_2}. \tag{5}$$

To avoid confusion, let us provide the definition of this quantity in greater detail.

Given M rings in the system with N monomers each, there are a total of $K = NM/s$ subchains or blobs. Consider one of them and let us call it A. n_{surf} is how many monomers of subchain A are in contact with monomers of any other subchain, where 'in contact' means within a distance less than r as described above. Each surface monomer is in contact with one or more monomers from other subchains, but it may be in contact with more than one monomer from more than one other subchain. Let us denote $z_1, z_2, \ldots, z_{n_{\text{surf}}}$ the number of 'foreign' contacts for each of the n_{surf} monomers. The sum of all these z_i is the total number of monomer–monomer contacts that our subchain A has with all other subchains. This sum can also be written as $n_{\text{surf}}\langle z\rangle$, where $\langle z\rangle$ is the average of all z_i. Let us make a list of other subchains $\{B_1, B_2, \ldots, B_Q\}$, which are thus in contact with subchain A. Here, two subchains are said to be 'in contact' if at least one monomer from one of them is in contact with at least one monomer of the other. Thus, $Q = Q(A)$ is the number of other subchains which are in contact with our subchain A. Now we can count monomer–monomer contacts of A with monomers of B_1, with monomers of B_2, etc. Let us call these numbers $Y_1, Y_2, \ldots, Y_Q$. The sum of all these Y_i must be equal to $n_{\text{surf}}\langle z\rangle$. Therefore, $n_{\text{surf}}\langle z\rangle/Q$ must be equal to the number of contacts between subchain A and its neighboring subchains, averaged over all neighboring subchains. We can denote it $n_{\text{blob}-\text{blob}}$ and then

$$n_{\text{blob}-\text{blob}}(s) = n_{\text{surf}}(s)\langle z(s)\rangle/Q(s). \tag{6}$$

In theory, for very large s, we assume that (1) Q and $n_{\text{blob}-\text{blob}}$ are statistically independent, (2) n_{surf} and $\langle z\rangle$ are statistically independent, and (3) Q and $\langle z\rangle$ are independent of s. Then we obtain $\beta_1 = \beta_2$, which yields $\beta + \gamma = 2$.

The simulation data for both off-lattice and lattice systems in regard to all these quantities are shown in figure 9. It is plausible, although there is no completely convincing evidence, that $Q(s)$, the number of neighbors on the coarse-grained blob level, saturates at large s. If that is the case, then it is also plausible that β_2 in the dependence of $n_{\text{blob}-\text{blob}}$ on s approaches a value very close to unity and, therefore, to β_1. However, we cannot rule out the possibility that $Q(s)$ reaches a maximum and then goes somewhat down. In any case, all the behaviors are remarkably similar for off-lattice and lattice models, including the high numerical value of $Q(s)$, up to about 60 or so.

What is clearly seen is that $n_{\text{blob}-\text{blob}}$ is not a power law over the observed interval of s, and its slope on double logarithmic axes increases continuously. Around $s/N_e = 1$ the slope is roughly 0.8, which is where $\gamma \approx 1.2$ is visible in figure 6, in agreement with the $\beta + \gamma = 2$ theorem.

Mathematically, the theorem $\beta + \gamma = 2$ holds for a fractal, e.g., the system with infinite range of scales. Melt of rings exhibits some fractal properties, but in many respects it exhibits unusually and unexpectedly broad finite size cross-over. At this point we cannot claim to understand this cross-over fully, but we believe that observations reported in our work lay the foundation for such understanding. In this regard, we observed $\beta_1 = 0.97$ very accurately through the entire range of scales examined. At the same time, determination of γ and β_2 is more tricky, because their finite size behavior is much more pronounced. In the range of s about 10^2 we find $\gamma \approx 1.2$ and $\beta_2 \approx 0.8$. In the light of the $\beta + \gamma = 2$ theorem this suggests that the finite size behavior of both β_2 and γ might have the same origin.

Finally, in light of the previous surface roughness discussion we can return to the static structure factor and the way it is plotted in figure 5. This plotting is motivated by the arguments

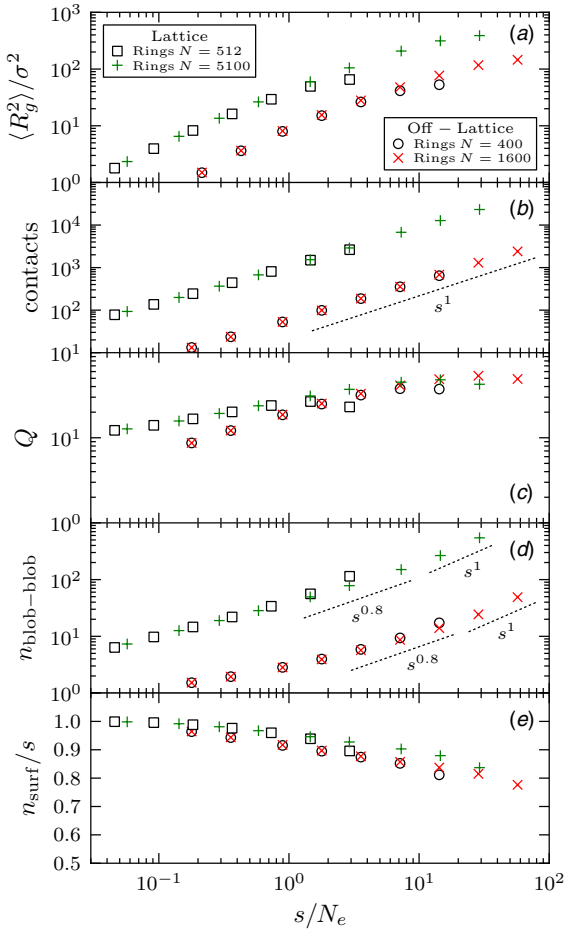

Figure 9. Several characteristics of subchains for off-lattice and lattice models. Data for rings of length $N = 400$ (circles) and $N = 1600$ (crosses) are shown for the off-lattice systems, while $N = 512$ (squares) and $N = 5100$ (pluses) are shown for the lattice systems. (a) Mean squared gyration radius reproduced from figure 4. (b) Total number of inter-subchain monomer contacts for the subchain as a function of subchain length s. Monomer contacts are defined as before by the cutoff length of $r = 2^{1/6}\sigma$ for off-lattice and $r = \sqrt{3}\sigma$ for the lattice systems. (c) The average number of subchains in contact with a given subchain of length s, $Q(s)$, as a function of s. At large s, the value $Q(s)$ appears to saturate. In the large s region, where $Q(s)$ saturates, the number of blob–blob contacts ($n_{\mathrm{blob-blob}}$) is approximately linear in s as shown in (d). This is consistent with equation (6) and with the expectation that $\beta_1 = \beta_2$ for very long subchains. Unfortunately, the data are such that it is not possible to determine whether β_2 is one or, as we suspect regarding β_1, a value slightly below unity. In the region around $s/N_e \sim 1$, where contact probability seems to exhibit scaling with $\gamma = 1.2$ (see figure 6), the blob–blob contacts data exhibit a slope close to 0.8, in accord with $\beta + \gamma = 2$. (*e*) The fraction of surface monomers of the subchain, defined by the same cutoff length as before, as a function of s. These are the same data as in figure 8, but plotted differently to emphasize that β_1 is likely to be slightly below unity.

given in [10] based on the work of Meyer *et al* [29]. The plotting involves the surface roughness exponent β. The argument behind it works well as long as both surface roughness exponents are the same, $\beta_1 = \beta_2$, and can be used interchangeably. The fact of the matter is that the best collapse of the static structure factor data for rings of various lengths is achieved with $\beta = 0.93$, both for off-lattice and lattice models.

To conclude, there is a very high degree of agreement between lattice and off-lattice simulation results for the concentrated system of nonconcatenated and unknotted rings. The simulations provide rather convincing proof that individual rings are quite seriously squeezed by the surrounding rings and get somewhat segregated from one another, forming territories. This segregation, however, does not lead to a simple compact structure as the analysis of the surface properties and the comparison to Moore curves demonstrate. Despite significant effort in data analysis, we gained so far only a rather preliminary understanding of the details of the scaling behavior in a more detailed description, including the surface roughness of folded rings and its relation to the contact probability scaling. In this paper, the data forced us to distinguish between two separate exponents, β_1 and β_2, each of which describes surface roughness in some way. For an idealized fractal model, these two have to be the same. What we observe in both lattice and off-lattice systems is that the power law involving β_1 (equation (3)) is obeyed very closely, while similar power law with β_2 (equation (6)) appears to be much less well-defined for the range of polymer lengths examined. The most likely interpretation of this puzzling observation is a finite size effect, but much effort will be required to understand the exact nature of it. If one adopts a different strategy and assumes from the outset that the two surface roughness exponents are the same, $\beta_1 = \beta_2 = \beta$, then the most sensitive determination of β is achieved from the fit of static structure factor, which yields $\beta = 0.93 \pm 0.02$. This complicated situation with our incomplete understanding of β exponents continues with contact probability exponent γ (which the reader should note has nothing to do with the other exponent involved in the determination of the total number of conformations for, e.g., a self-avoiding walk). The $\beta + \gamma = 2$ theorem is valid under the assumption of unique β. In a forthcoming paper [30] we relax this assumption and establish the relations between all three exponents β_1, β_2, and γ. Nevertheless, our understanding is still not complete.

Despite the difficulties in understanding the model system of nonconcatenated rings, we must also think of a much bigger problem of how our results are relevant to chromosomes. We discuss this problem in great detail in [30]. Here we will only say that recent quantitative experiments for a variety of organisms [1–3, 31], combined with the puzzling observation of chromosome territories [32], are naturally interpreted in favor of fractal models with topological constraints. Therefore, detailed analysis of internal consistency and difficulties in understanding such models is the necessary step towards uncovering the riddle of the genome folding mechanism. This is what we have attempted in this paper.

Acknowledgments

The authors are grateful to Gary Grest for numerous inspiring discussions and to Thomas Vettorel and Won Bo Lee for fruitful collaboration at early stages of our project on ring polymers. We thank Jan Smrek for providing the Moore curves. This research was supported in part by the National Science Foundation under grant no. NSF PHY11-25915. KK and AYG acknowledge the hospitality of KITP Santa Barbara where part of this work was completed. Research carried out in part at the Center for Functional Nanomaterials, Brookhaven National Laboratory, which is supported by the US Department of Energy, Office of Basic Energy Sciences, under contract no. DE-AC02-98CH10886.

References

[1] Lieberman-Aiden E *et al* 2009 Comprehensive mapping of long-range interactions reveals folding principles of the human genome *Science* **326** 289–93

[2] Duan Z, Andronescu M, Schutz K, McIlwain S, Kim Y J, Lee C, Shendure J, Fields S, Blau C A and Noble W S 2010 A three-dimensional model of the yeast genome *Nature* **465** 363–7
[3] Zhang Y, McCord R, Ho Y-J, Lajoie B, Hildebrand D, Simon A, Becker M, Alt F and Dekker J 2012 Spatial organization of the mouse genome and its role in recurrent chromosomal translocations *Cell* **148** 908–21
[4] Mirny L A 2011 The fractal globule as a model of chromatin architecture in the cell *Chromosome Res.* **19** 37–51
[5] Rosa A and Everaers R 2008 Structure and dynamics of interphase chromosomes *PLoS Comput. Biol.* **4** e1000153 08
[6] Kapnistos M, Lang M, Vlassopoulos D, Pyckhou-Hintzen W, Richter D, Cho D, Chang T and Rubinstein M 2008 Unexpected power-law stress relaxation of entangled ring polymers *Nature Mater.* **7** 997–1002
[7] Milner S T and Newhall J D 2010 Stress relaxation in entangled melts of unlinked ring polymers *Phys. Rev. Lett.* **105** 208302
[8] Vettorel T and Kremer K 2010 Development of entanglements in a fully disentangled polymer melt *Macromol. Theory Simul.* **19** 44–56
[9] Vettorel T, Grosberg A Y and Kremer K 2009 Statistics of polymer rings in the melt: a numerical simulation study *Phys. Biol.* **6** 025013
[10] Halverson J D, Lee W B, Grest G S, Grosberg A Y and Kremer K 2011 Molecular dynamics simulation study of nonconcatenated ring polymers in a melt: I. Statics *J Chem. Phys.* **134** 204904
[11] Halverson J D, Lee W B, Grest G S, Grosberg A Y and Kremer K 2011 Molecular dynamics simulation study of nonconcatenated ring polymers in a melt: II. Dynamics *J. Chem. Phys.* **134** 204905
[12] Halverson J D, Grest G S, Grosberg A Y and Kremer K 2011 Rheology of ring polymer melts: from linear contaminants to ring/linear blends *Phys. Rev. Lett* **108** 038301
[13] de Gennes P-G 1979 *Scaling Concepts in Polymer Physics* (Ithaca, NY: Cornell University Press)
[14] Mandelbrot B B 1982 *The Fractal Geometry of Nature* (New York: Freeman)
[15] Sagan H 1994 *Space-Filling Curves* (Berlin: Springer)
[16] Everaers R, Sukumaran S K, Grest G S, Svaneborg C, Sivasubramanian A and Kremer K 2004 *Science* **303** 346
[17] Carmesin I and Kremer K 1988 *Macromolecules* **21** 2819
[18] Kremer K and Grest G S 1990 Dynamics of entangled linear polymer melts: a molecular-dynamics simulation *J. Chem. Phys.* **92** 5057–86
[19] Cates M E and Deutsch J M 1986 Conjectures on the statistics of ring polymers *J. Phys.* **47** 2121–8
[20] Hur K, Jeong C, Winkler R G, Lacevic N, Gee R H and Yoon D Y 2011 *Macromolecules* **44** 2311–5
[21] Suzuki J, Takano A, Deguchi T and Matsushita Y 2009 *J. Chem. Phys.* **131** 144902
[22] Brown S and Szamel G 1998 *J. Chem. Phys.* **109** 6184
[23] Müller M, Wittmer J P and Cates M E 1996 *Phys. Rev.* E **53** 5063
[24] Grosberg Alexander Y and Khokhlov Alexei R 1994 *Statistical Physics of Macromolecules* (New York: American Institute of Physics Press)
[25] Wittmer J P, Meyer H, Baschnagel J, Johner A, Obukhov S, Mattioni L, Müller M and Semenov A N 2004 Long range bond-bond correlations in dense polymer solutions *Phys. Rev. Lett.* **93** 147801
[26] Wittmer J P, Beckrich P, Meyer H, Cavallo A, Johner A and Baschnagel J 2007 Intramolecular long-range correlations in polymer melts: the segmental size distribution and its moments *Phys. Rev.* E **76** 011803
[27] Wittmer J P *et al* 2011 Scale-free static and dynamic correlations in melts of monodisperse and flory-distributed homopolymers. A review of recent bond-fluctuation studies *J. Stat. Phys.* **145** 1017–126
[28] Hsiao-Ping H, Paul W and Binder K 2011 *Europhys. Lett.* **95** 68004
[29] Meyer H, Wittmer J P, Kreer T, Johner A and Baschnagel J 2010 Static properties of polymer melts in two dimensions *J. Chem. Phys.* **132** 184904
[30] Halverson J, Smrek J, Kremer K and Grosberg A Y 2012 From melt of rings to chromosome territories: the role of topological constraints in genome folding in preparation
[31] Sexton T, Yaffe E, Kenigsberg E, Bantignies F, Leblanc B, Hoichman M, Parrinello H, Tanay A and Cavalli G 2012 Three-dimensional folding and functional organization principles of the drosophila genome *Cell* **148** 458–72
[32] Cremer T, Cremer M, Dietzel S, Müller S, Solovei I and Fakan S 2006 Chromosome territories—a functional nuclear landscape *Curr. Opin. Cell Biol.* **18** 307–16